Published by Elsevier Science Ltd 1996
Paper No. 1242. (quote when citing this article)
Eleventh World Conference on Earthquake Engineering
ISBN: 0 08 042822 3

A STUDY ON AMPLIFICATION FACTORS OF EARTHQUAKE MOTIONS OBSERVED AT A GRANITE SITE AND RELATIONSHIPS BETWEEN THEIR VERTICAL AND HORIZONTAL MOTIONS

KEN'ICHI ABE
Dept. of Nuclear Power & Energy, Kumagai-gumi Co., Ltd. ,2-1 Tsukudo-cho
Shinjuku-ku Tokyo 162 Japan

HIROYUKI WATANABE
Dept. of Civil and Environmental Engineering, Saitama Univ., 255 Shimookubo Urawa
Saitama Pref. Japan

ABSTRACT

In order to clarify the site amplification factors and the relationships between their horizontal and vertical motions on a granite site regarded as a basin, we examine two kinds of spectral ratios using observed motions obtained from a vertical array observation system on its site. One is obtained by ratios between particular two points on and in the granite site, the other is by ratios of the vertical components to the horizontal ones at the points respectively. We compare the two kinds of spectral ratios with the theoretical estimations based on Silva's method in which inelastic layers on an elastic half-space are considered, and conclude that occurrences of vertical motions after the arrival of S-wave are strongly affected by the deep ground structure over the depth of 4 kilometers and the incident angles to the deep half-space.

KEYWORDS
Granite Site; Vertical Array; Amplification Factor; Vertical Motion; Deep Ground Structure; Incident Angle

INTRODUCTION

The authors have set up a vertical array observation system on a granite site to research the characteristics of motions in and on a rock site. The site, S-4, on an outcrop of granite layer in Shibata, Miyagi Pref., is one of the sites that constitute the array observation system named "KASSEM" (Shimizu *et al.*, 1988). We added the new observation point, S-4D, in the granite layer and have observed ground motions since 1991. Although the site is geologically considered to be on the outcrop of the granite layer in which the deepest observation point of "KASSEM" exists and is also generally regarded to indicate amplification characteristics of a basin, it is probable that the influence by weathered layers on surface can not be ignored.

In order to clarify the site amplification factors and the relationships between their horizontal and vertical motions on the site regarded as a basin, we examine two kinds of spectral ratios using observed motions of 10 events. One is obtained by ratios between particular two points on and in the granite site, the other is by ratios of the vertical components to the horizontal ones at the points respectively. We compare the two kinds of spectral ratios with the theoretical estimations based on Silva's method in which inelastic layers on an elastic half-space are considered, and examine the amplification factors and the spectral ratios of the vertical components to the horizontal one relating to the ground structure and the incident angle.

SITE INVESTIGATION AND ARRAY OBSERVATION SYSTEM

Site Investigation

We investigated the elastic velocity structure by means of PS logging toward the depth of 50 meters in the bore hole as well as the density structure by means of gamma-ray. The results are shown in Fig. 1. The S-wave velocities of the layer in which weathering progresses decrease to around 1.0 km/sec by the depth of 23.5 meters and indicates 2.4 km/sec under its depth. On the basis of the investigation, the elastic velocity structure and the density structure are constructed as shown in Fig. 2. Here, the ground structure under the depth of 50 meters is assumed to be equivalent to the deep ground structure of Tohoku region in the northern part of Japan(Den, 1967).

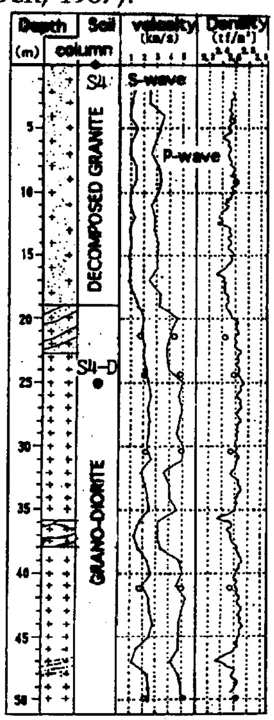

Fig.1. Results of PS logging and density by means of gamma-ray Circular plots show values from test piece.

depth	ρ [t/m³]	V_s [m/s]	V_p [m/s]	Q_s (the standard ground model, V_s / 32)	Q_p (the standard ground model)	Q_s (the deep ground model, V_s / 32)	Q_p (the deep ground model)
S-4 0.0 – 18.5	2.51	1,150	2,950	36	180	36	180
18.5 – 23.5	2.58	1.930	3,930	60	300	60	300
23.5 – S-4-D 25.0	2.65	2.400	4,500	75	375	75	375
25.0 – (1,000)	2.65	2,400	4,500	—	—	75	375
(1,000) – (4,000)	(2.65)	(3,000)	(5,500)			94	470
(4,000) –	(3.00)	(3,300)	(6,000)				

Fig.2. The elastic velocity structure and the density structure

Array Observation System

An acceleration seismograph of three components (NS, EW, UD) was set at the depth of 25 meters in non-weathered rock constituting a vertical array with seismograph set previously on the outcrop. The depth location of the seismographs is shown in Fig. 2 with the velocity structure. The seismograph SA-375CT manufactured by Tokyo Sokusin Co. Ltd,. indicates the characteristic data as shown in Table 1. The digital data of waves are recorded in the IC card system which have the data capacity of 25 minutes in the case that analog to digital conversion rate is 200 samples per second.

Table 1. Specification of used sensors

Sensor	Type	Full Range	Freq. Range	Amplitude Deviation	Freq. Deviation	sensitivity	Resonance Freq.	Damping Fac.
SA-375 CT	Survo Type	± 1000 *gal*	0.1 – 30 *Hz*	± 2.0%	± 5.0%	15μ*A* / *gal*	5 Hz	100

COMPARISON OF SPECTRAL RATIOS

Observed Spectral Ratios

We use the ground motions of 10 events observed from January 1992 to January 1993 as shown in Table 2. Fig.3 shows epicenters for the data set, and Fig. 4 shows the observed motions on the Off Kushiro event as an example. Here, the horizontal component of the waves, both NS and EW direction, is transformed into a wave toward the direction of the epicenter. Using both horizontal and vertical acceleration time histories simultaneously starting at the arrival of S-wave and ending at the duration time defined by eq. (1) (Hisada et al.,1978) from the arrival, we calculate velocity response spectra of which damping coefficient is zero because they are nearly equivalent to Fourier amplitude spectra of acceleration(Hudoson,1979).

$$T_d = 10^{0.31M - 0.774} \tag{1}$$

Table 2. Data of events

Event No	Name	N. L (deg.)	Long. E (deg.)	Depth (km)	Mag.	Distance (deg)
1	Center of Yamagata Pref.	38.42	140.53	121	5.7	43
2	Earst off Fukushima Pref.	36.88	141.35	67.6	4.7	142
3	Earst off Fukushima Pref.	37.45	141.03	74	4.5	74
4	Earst off Ibaragi Pref.	36.67	141.26	43.8	5.7	163
5	Far Earst off Sanriku	39.38	143.67	0	6.9	292
6	Earst off Fukushima Pref.	37.55	141.05	76	4.7	88
7	Earst off Miyagi Pref.	38.15	141.75	52.8	4	87
8	Off Miyagi Pref.	38.93	142.55	33.5	5.9	183
9	Off Miyagi Pref.	38.93	142.57	32	5.7	185
10	Off Kushiro	42.85	144.38	107	7.8	614

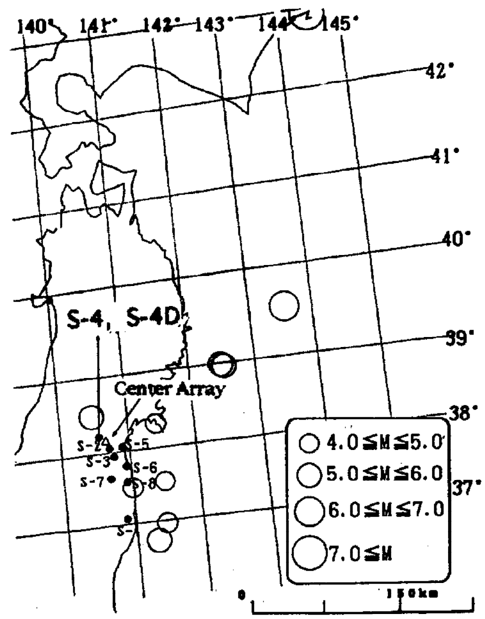

Fig.3. Epicenters and observation sites

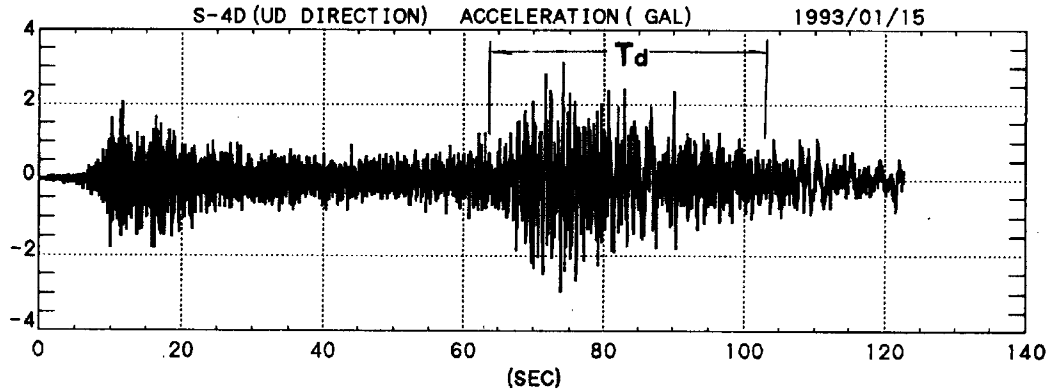

Fig.4. An example of observed motions

Concerning the mean ratios on spectra due to 10 events, Fig. 5(a) shows the spectral ratios of the S-4D point to the S-4 point in both horizontal and vertical directions and Fig. 5(b) shows the spectral ratios of vertical component to horizontal one at the points respectively. As shown in Fig.5(a), the ratios on both horizontal and vertical components tend to amplify substantially in the period range less than 0.2 seconds; horizontal ratios indicate the peak period at 0.07 seconds and vertical ratios have it at 0.035 seconds. In Fig. 5(b), both ratios of vertical component to horizontal one coincide with each other in period range greater than 0.2 seconds. These ratios vary substantially in the period range less than 0.2 seconds as well as the ratios on amplification; the ratios on the S-4 point indicate the off-peak period at 0.08 seconds and these on the S-4D point have the peak period at 0.07 seconds, the off-peak period at 0.035 seconds. On the S-4 point, the ratios of vertical component to horizontal one tend to vary due to the deviations of the amplification ratios between horizontal and vertical components. We calculated the ratios of vertical component to horizontal one on the amplification ratios as shown in Fig.5(a) and illustrated it with the ratios on the S-4 point in Fig. 5(b). Although both ratios are similar in shape, these values are not entirely in agreement with each other, so that the appreciable deviation between both ratios as shown in Fig. 5(b) consequently agrees with the ratios on the S-4D point.

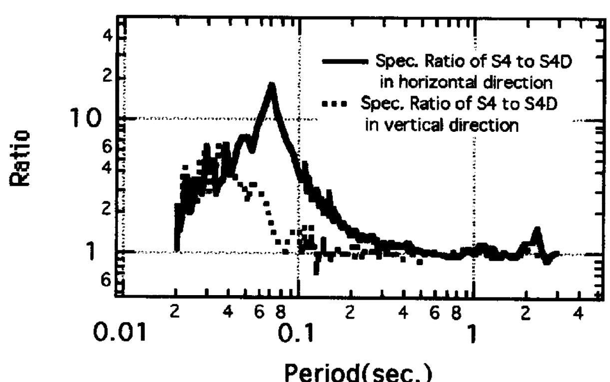

Fig.5(a). Mean spectral ratios of S-4 to S-4D

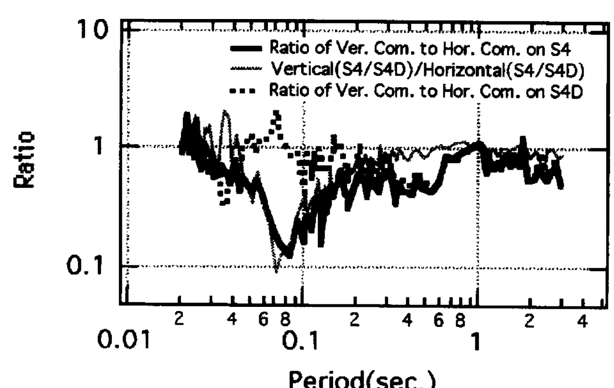

Fig.5(b). Mean spectral ratios of vertical component to horizontal one

<u>Comparison with Theoretical Spectral Ratios</u>

We compare the observed spectral ratios with the theoretical estimations based on Silva's method in which inelastic layers on an elastic half-space are considered(Abe,1990). If motions are composed of body waves, the theoretical ratios should be estimated in the case of obliquely incident SV-wave to the layers. Two kinds of ground structure model are considered because of the difference on the half-space level. One is called the standard ground model in which one layer structure is constructed over a half-space at the depth of 25 meters. The other is the deep ground model in which a multi-layer's structure is constructed over a half space at the depth of 4 kilometers. These model constants are shown in Fig. 2. The Qs values are estimated by the following equation (Architecture Institute of Japan,1987) and the Qp values are assumed as five times of the Qs values.

$$Qs=Vs/32 \tag{2}$$

where Vs presents S-wave velocity (meter per second).
Using the above two kinds of models as changing incident angles, we calculate theoretical ratios between two points on and in the granite site corresponding to observed ratios as shown in Fig. 6. The estimated ratios by the standard model are inclined to be similar to observed ratios as these incident angles become close to zero. Although the estimated ratios by the deep ground model do not vary substantially as incident angles change, in particular, theoretical ratios in vertical direction give better estimation for observed ratios than ones by the standard model.

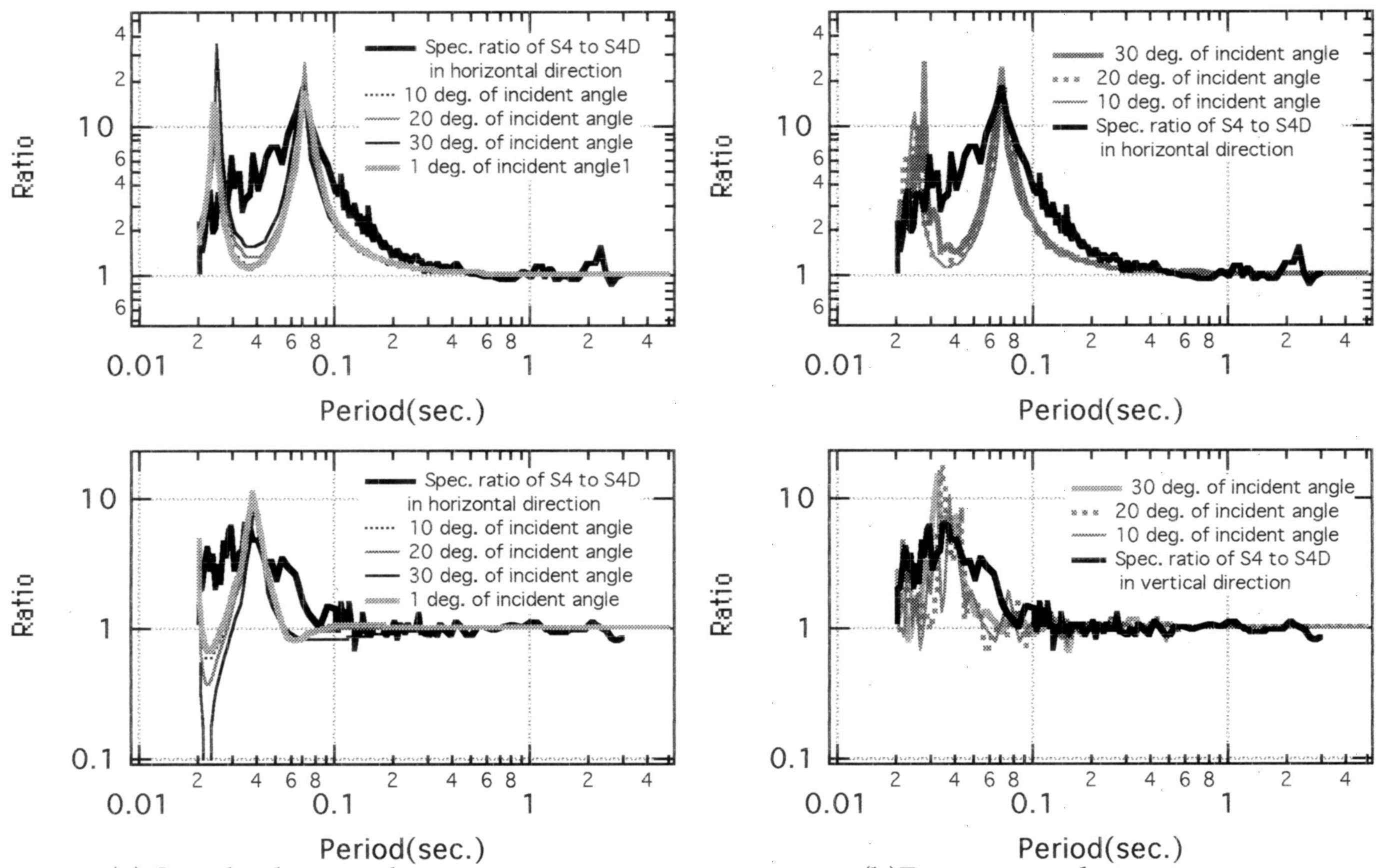

(a) Standard ground structure (b)Deep ground structure

Fig.6. Comparison between two kinds of model on spectral ratio of S-4 to S-4D

Concerning observed ratios of vertical component to horizontal one, we make the same comparison in Fig. 7. In comparison with the estimated ratios by the standard model, the estimated ratios are not in good agreement with the observed ratios on the S-4 point although the ratios at the incident angles of 10 degrees are similar at the point of the concave shape and the ratios at the incident angle of 30 degrees are close in ratio value. On the other hand, the estimated ratios by the deep ground model at the incident angle of 30 degrees are appreciably similar in both shape and value to observed ratios on the S-4 point. Next, we contrast the estimated ratios by two models with the observed ratios on the S-4D point as shown in Fig. 7 (b) where the ratios by the standard model are given at the incident angle of 10 degrees and ones by the deep ground model are at the incident angle of 30 degrees. Though the ratios by the standard model present the ratio shape in the short period range less than 0.2 seconds, both are not similar in ratio value. The application of the deep ground model, in particular, in the case of incident angle of 30 degrees, improves appreciably the ratio similarity in shape and value. The above examinations show that in order to make the observed values of ratios agree with the theoretical values we must estimate the ratios by the deep ground model at the incident angle of 30 degrees.

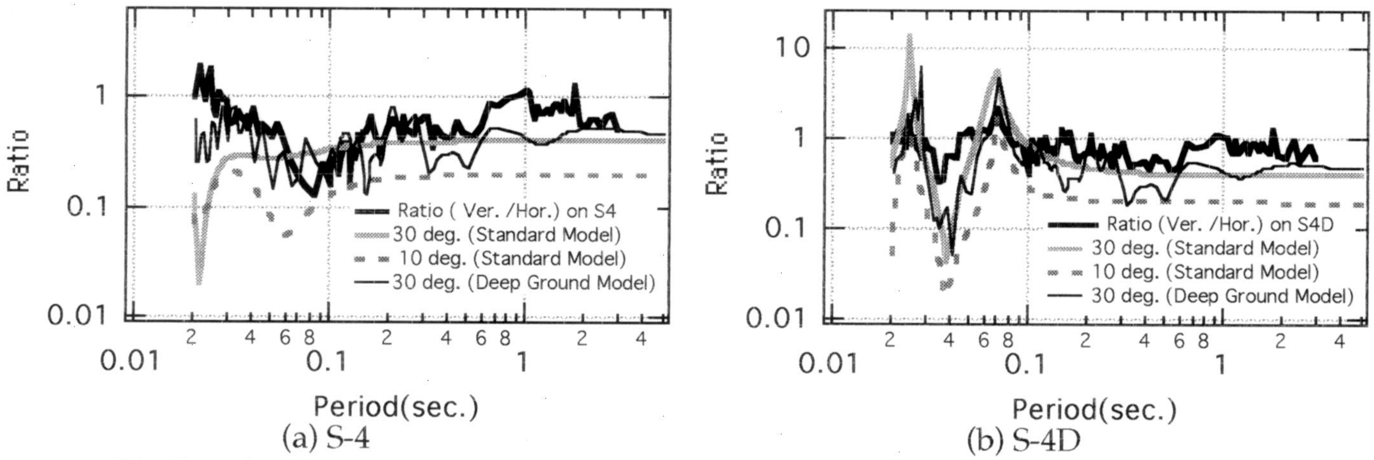

Fig.7. Comparison on spectral ratios of vertical component to horizontal one

CONCLUSIONS

As earthquake motions propagate near the surface, incident angles at the boundaries of layers are on the decrease. However, the observed spectral ratios of the vertical components to the horizontal ones on outcrop disagree theoretical ones by modeling the surface layer at smaller incident angles as well as the vertical ratios between on and in the ground. These ratios are explained by the fact that S-waves change to P-waves or P-waves to S-waves at the boundaries of layers during propagation from the depth of 4 kilometers. Therefore, it can be concluded that occurrences of vertical motions after the arrival of S-wave are strongly affected by both the deep ground structure and the incident angle to the deep half-space.

REFERENCES

Abe, K., M. Terada, K. Kasuda and T. Shimizu (1990). Estimation of amplification spectra for P and SV waves, Proc. of 2nd Int. Conf. on Recent Advances in Geotech. E. E. and Soil Dynamics, Vol.2-1229-1235.

Architectural Institute of Japan (1987). Seismic Loading — State of the art and future developments—, 119 (in Japanese).

Den, N. (1967). The earth's crust structure on the sea area around Japan, Zisin, 20, (4), 131-134 (in Japanese).

Hudson, D. (1979). Reading and interpreting strong motion accelerograms, Earthquake Engineering Research Institute, 55-60.

Hisada, T., Y. Ohsaki, M. Watabe, and T. Ohta (1978). Design spectra for stiff structures on rock, Proc. 2nd Int. Conf. on Microzonation, 1187-1198.

Shimizu, T., K. Abe, K. Kasuda and E. Yanagisawa (1988). The development of the dense instrument array system KASSEM and the analysis of observed earthquake waves. Proc. 9th World Conf. Earthq. Eng., Vol. 8-137-142.

Silva, W. (1976). Body waves in a layered anelastic solid. Bull. Seismol. Soc. Am. Vol.66, No.5, 1539-1554